32nd EPS Conference on Plasma Phys. Tarragona, 27 June - 1 July 2005 ECA Vol.29C, O-1.001 (2005)

The Role of the m/n=3/2 Tearing Mode in the Hybrid Scenario in DIII-D

P.A. Politzer[1], M.E. Austin[2], D.P. Brennan[3], T.A. Casper[4], M.S. Chu[1], J.C. DeBoo[1], E.J. Doyle[5], M.E. Fenstermacher[4], J.R. Ferron[1], C.M. Greenfield[1], A.W. Hyatt[1], R.J. Jayakumar[4], R.J. La Haye[1], C. Kim[6], T.C. Luce[1], G.R. McKee[6], M. Murakami[7], T.W. Petrie[1], C.C. Petty[1], R. Prater[1], T.L. Rhodes[5], M.R. Wade[1], G. Wang[5], and A.S. Welander[1]

[1]*General Atomics, San Diego, California, USA*
[2]*Universxity of Texas, Austin, Texas, USA*
[3]*Massachusetts Institute of Technology, Cambridge, Massachusetts, USA*
[4]*Lawrence Livermore National Laboratory, Livermore, California, USA*
[5]*University of California, Los Angeles, California, USA*
[6]*University of Wisconsin, Madison, Wisconsin, USA*
[7]*Oak Ridge National Laboratory, Oak Ridge, Tennessee, USA*

The DIII-D realization of the proposed ITER hybrid scenario has a small, stationary m/n = 3/2 NTM associated with it. These plasmas, with $q_{95} > 4$, also show $q_0 \geq 1$ and no sawteeth (or very small sawteeth for $q_{95} \approx 4$). We conjecture that one effect of the 3/2 NTM is to regulate the central value of q, via the rapid increase in the $m/n = 2/2$ sideband as $q_0 \rightarrow 1$. We present evidence for the coupling between the 3/2 mode island width and q_0, and discuss possible physical mechanisms connecting the NTM and the current profile.

The hybrid scenario has been proposed as a robust tokamak operating scenario for high performance operation of ITER [1]. The purpose is to provide the maximum neutron fluence per ITER pulse. In its performance characteristics it is intermediate between the standard, high current, ELMy H-mode scenario [2] and the steady-state Advanced Tokamak scenarios [3]. The hybrid plasma is stationary – profiles of density, temperature, and current do not change with time – but not steady-state because the transformer provides a significant fraction of the current. Projections to ITER based on DIII-D experiments indicate that a pulse length longer than one hour should be achievable, with a power gain $Q \geq 10$ [4,5].

Compared to the standard, ELMy H-mode, the hybrid scenario provides better confinement at the same current, or equivalent confinement at lower current. Using the latter condition reduces the transformer requirements and allows longer pulse length. The scenario also allows stable operation to a higher level of β, yielding higher gain (Q). Several realizations of the hybrid scenario have been reported (DIII-D, ASDEX-U [6], JET [7], and JT-60U) [8]. We will focus on characterization and on the physical mechanisms of the DIII-D realization.

In order to confidently extrapolate the hybrid scenario to ITER operation, it is important to develop a better understanding of the physical mechanisms linking the equilibrium configuration, MHD stability, and turbulence. We have demonstrated that an improved stationary state exists, and have shown that it can be produced over a wide range of basic plasma parameters. The next step is to understand the processes which sustain this state so that reliable predictive models can be developed.

The DIII-D program has done extensive studies of the operating regime for the hybrid scenario [5]. In DIII-D, hybrid operation is characterized by $q_{95} \geq 4$. J(0) is lower and q_0 is higher than is expected for comparable conventional scenario plasmas. q_0 is generally above, but very close to unity: $q_0 = 1 + \varepsilon$ with $\varepsilon \le 0.05$. Sawteeth are either absent ($q_{95} > 4$) or barely detectable ($q_{94} \approx 4$), and have no noticeable effect. The reduced sawtooth amplitude reduces or eliminates a trigger for the deleterious $m = 2$, $n = 1$ neoclassical tearing mode. The 2/1 mode limits the achievable beta in the conventional H-mode scenario. Hybrid plasmas show good confinement, with $H_{89\rho}$ up to 2.8 and H_{98y2} up to 1.7 [9]. The improvement in confinement above standard ELMy H-mode is a consequence of reduced transport over the entire cross-section, rather than a local reduction characteristic of an ITB.

A key feature of the hybrid scenario in DIII-D is the presence of an $m = 3$, $n = 2$ neoclassical tearing mode (NTM). We conjecture that this nonlinearly saturated mode is responsible for modification of the J and q profiles so as to improve the beta limits and the confinement. In this paper, we examine the characteristics of the 3/2 NTM, and discuss several possible mechanisms that may link the NTM to the current profile. We focus our attention on the interaction between the 3/2 NTM, J(ρ) near the magnetic axis, and the reduction or elimination of sawteeth. The examination of the effect of the 3/2 NTM on the q-profile in the outer half of the plasma, and possible advantageous effects on confinement will be discussed in future publications.

The key to producing a hybrid plasma in DIII-D is to raise β early in the discharge evolution. This initiates an early H-mode, minimizes the ELM-free period, and triggers a 3/2 NTM before q_0 falls to 1 and sawtoothing begins (Fig. 1). If the sawteeth are allowed to start, a standard H-mode configuration results. With the 3/2 mode, the current density is maintained at the level needed to keep q_0 just above 1. An understanding of the hybrid scenario requires an explanation for the regulation of q_0 at this particular value.

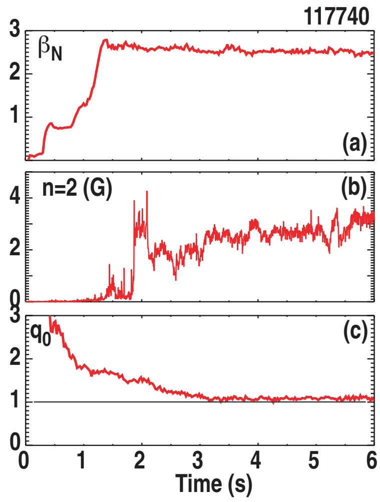

Fig. 1. Evolution of a hybrid scenario discharge in DIII-D. (a) Normalized $\beta_N = \beta(\%)aB/I(MA)$. (b) The rms amplitude at the Mirnov probes of the n=2 toroidal harmonic, as generated by the 3/2 NTM. (c) The safety factor on the magnetic axis.

This observation is not coincidental. Calculation of the components of the current profile indicates that the known contributions from the Ohmic, bootstrap, and neutral beam driven currents add up to more than is observed, with the excess inside the $q = 3/2$ surface (Fig. 2). This is confirmed by simulations of the current profile evolution using the observed profiles as initial conditions: the computed current becomes significantly more peaked at the axis with time.

Both the observed and calculated structure of the NTM indicate that it can be responsible for the regulation of q_0 (Fig. 3). We are able to measure both δn_e and δT_e associated with the NTM. Near the $q = 1.5$ surface, on the outboard side, both $\delta n_e / n_e$ and δT_e show the expected island amplitude and phase signatures. In this experiment, the δn_e diagnostic has finer spatial resolution but covers a smaller region. The δT_e measurement also shows the island structure on the inboard side of the axis, with small amplitude and a phase corresponding to the odd ($m = 3$) poloidal mode number. Near the axis, δT_e is about 1/3 of the peak value at the 3/2 island, and lags the peak near the island by about $2\pi/3$.

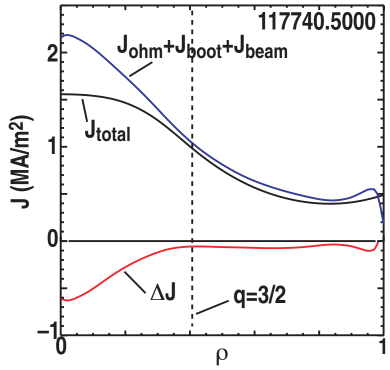

Fig. 2. Components of the current profile, averaged for 0.5 s in a stationary plasma. The total current (J_{total}; black) is obtained from EFIT equilibrium reconstruction including MSE. The computed current (J_{ohm}+J_{boot}+ J_{beam}; blue) is calculated using the measured n_e, T_e, T_i, and Z_{eff} profiles. The sum is the expected current profile. The difference (ΔJ; red) is the non-classical current attributed to the presence of the 3/2 NTM. The total non-classical current inside the q = 1.5 surface (dashed line) is ≈50 kA.

The experimental connection between the 3/2 mode and the value of q_0 is shown in Fig. 4. Electron cyclotron current drive (ECCD) localized at the $q = 1.5$ surface is used to either suppress the 3/2 NTM (co-ECCD) or enhance the mode (counter-ECCD). Before the ECCD, the width of the 3/2 island $w_{3/2}$ is 0.05 m. These plasmas have $q_{95} \approx 4.1$, and have small sawteeth. When the NTM width is reduced to the noise level, $\Delta q_0 \approx -0.02$; the sawtooth amplitude increases and the frequency decreases. When the island width is increased to 0.085 m, $\Delta q_0 \approx +0.05$; the sawtooth amplitude drops and the frequency increases. This dependence of q_0 on $w_{3/2}$ will serve as a test of future nonlinear models of this interaction.

The connection between the 3/2 mode and q_0 is made by noting that the NTM is a global mode. Although the largest feature is the island chain at $q = 1.5$, there are m = 2,4,5,… spatial sidebands, which have a kink-like structure. This is illustrated by linear calculations using PEST3 [10] and NIMROD [11]. In Fig. 5, we have plotted two model PEST3 cases, with q_0 = 1.008 and q_0 = 1.03. There

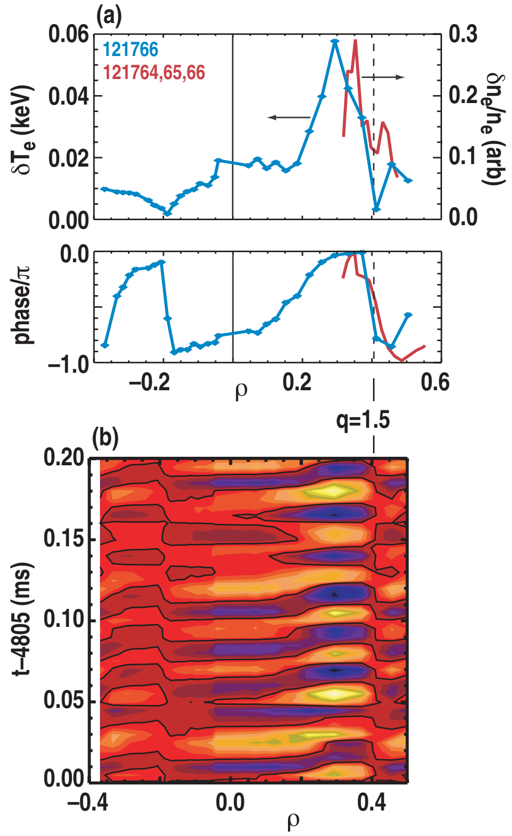

Fig. 3. (a) Amplitude and phase of δT_e (blue) and $\delta n_e/n_e$ (red) vs ρ. (b) Contour level plot of δT_e vs ρ and time for an 0.2 ms interval during the stationary period. In addition to the dominant m/n=3/2 island at the q = 1.5 surface, there is coherent structure near the axis which has the characteristics of the 2/2 spatial sideband.

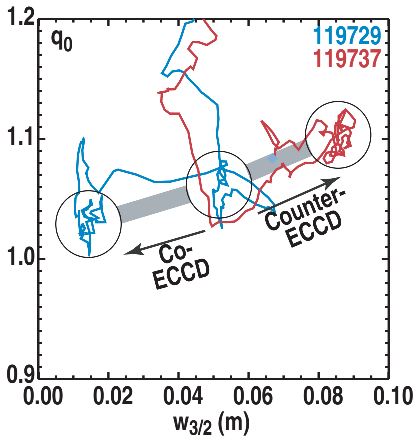

Fig. 4. Time evolution of the central safety factor (q_0) and the width of the m/n=3/2 island ($w_{3/2}$) for two discharges. In both cases, q_0 initially decreases while $w_{3/2}$ remains at ~0.055 m. In one discharge (blue) co-ECCD is used to suppress the NTM to the noise level, a reduction of q_0 by –0.03. In the other discharge, counter-ECCD is used to increase the width of the 3/2 island, with an increase in q_0 of +0.05.

is no difference in the radial structure of the poloidal harmonics except for the $m = 2$. As $q_0 \rightarrow 1$, the amplitude of the 2/2 sideband near the axis increases rapidly. This is not unexpected as the $q_0 = 1$ resonant condition is approached.

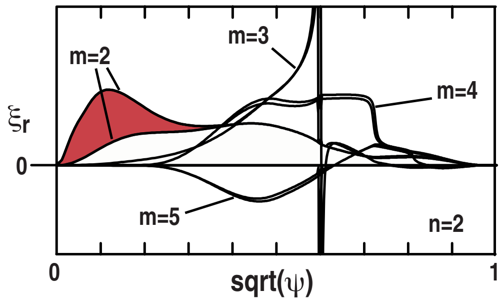

Fig. 5. PEST3 calculation of the poloidal harmonics associated with the n=2 toroidal mode, for two values of q_0: 1.03 and 1.008. The only significant difference is the increase in amplitude of the m=2 spatial sideband near the magnetic axis for the lower value of q_0.

Another piece of the puzzle is the mechanism whereby the current density at the axis is regulated. Several possibilities are associated with the 2/2 sideband of the 3/2 NTM: there may be a direct current drive associated with this perturbation, or the presence of a helical field perturbation near the axis increases the parallel resistivity (reducing the Ohmic current) and increases radial transport, particularly of fast ions (reducing the neutral beam current drive). To look for an effect on the radial transport of fast ions, we have looked at the neutron rate. A sudden change in the fast ion distribution should be reflected in a sudden change in neutron production, but no such effect is seen. If the beam-driven current is being modified, the effect is local and thus not detectible in the neutron production. Another proposed mechanism under study is the transport of poloidal flux out of the central region because of cyclic reconnection of the 3/2 island. The 3/2 amplitude is modulated by ELMs, with a rapid drop and a slower recovery. This time-asymmetric behavior may lead to flux pumping and reduction of the time-average central current density, analogous to sawteeth. However, there is no clear association between this mechanism and $q_0 = 1$.

In the DIII-D realization of the hybrid tokamak operating scenario, an $m = 3$, $n = 2$ NTM acts to modify the current profile in a beneficial way. In the core of the plasma, the current density is reduced, raising q_0 to just above 1, resulting in elimination of sawteeth (for $q_{95} >$ 4) or reduction of the sawtooth amplitude to an inconsequential level (for $q_{95} \approx 4$). This eliminates a trigger for the deleterious $m = 2$, $n = 1$ NTM. The regulation of q_0 at a level near 1 is a consequence of the resonant behavior of the amplitude of the 2/2 sideband of the 3/2 NTM, which grows rapidly as $q_0 \rightarrow 1$. Several candidates for the physical process connecting the 2/2 sideband and the current profile have been identified and are being investigated.

This work was supported by the U.S. Department of Energy under DE-FC02-01ER54698, W-7405-ENG-48, DE-FG03-01ER54615, DE-FG03-96ER54373, and DE-AC05-00OR22725.

[1] T.C. Luce, *et al*., Nucl. Fusion **41,** 1585 (2001).
[2] R. Aymar, *et al*., Plasma Phys. Controlled Fusion **44,** 519 (2002).
[3] T.S. Taylor, *et al*., Plasma Phys. Controlled Fusion **39,** B47 (1997).
[4] T.C. Luce, Nucl. Fusion **43,** 321 (2003).
[5] M.R. Wade, *et al*., Nucl. Fusion **45** 407 (2005).
[6] A.C.C. Sips, *et al*., Plasma Phys. Controlled Fusion **44,** B69 (2002).
[7] E. Joffrin, *et al*., Plasma Phys. Controlled Fusion **45,** A367 (2003).
[8] A. Isayama, *et al*., Nucl. Fusion **43,** 1272 (2003).
[9] ITER Physics Basis, Editors, Nucl. Fusion **39,** 2137 (1999).
[10] A. Pletzer, *et al*., J. Comput. Physics **115,** 530 (1994).
[11] C.R. Sovinec, *et al.,* J. Comput. Physics **195,** 355 (2004).